Graphene grown on Co(0001) films and islands: Electronic structure and its precise magnetization dependence

A. Varykhalov and O. Rader
Helmholtz-Zentrum Berlin für Materialien und Energie, Elektronenspeicherring BESSY II, Albert-Einstein-Str. 15, D-12489 Berlin, Germany

(Received 28 January 2009; revised manuscript received 17 May 2009; published 31 July 2009)

We achieve epitaxial growth of graphene on the ferromagnetic substrate Co(0001) by chemical vapor deposition using propylene. Structural and electronic properties are revealed by means of low-energy electron diffraction, scanning tunneling microscopy, and spin- and angle-resolved photoelectron spectroscopy. The results are compared to those of graphene/Ni(111) for which a magnetization-dependent Rashba effect has recently been reported. Bulklike Co(0001) films on W(110) can be separated into islands by heating, and subsequently they can be covered by graphene. Such system is used to present unambiguous proof that in graphene/Co(0001) there is no Rashba effect and no intrinsic dependence of the band dispersion on the magnetization occurs. The high spin polarization of secondary electrons reported for graphene/Ni(111) is confirmed for graphene/Co(0001) with higher values (~25%) due to the larger magnetic moment of Co.

DOI: 10.1103/PhysRevB.80.035437 PACS number(s): 79.60.Dp, 81.05.Uw, 73.20.At, 71.70.Ej

I. INTRODUCTION

Graphene, i.e., a single atomic layer of graphite has evolved as one of the most attractive topics in solid-state physics since its successful preparation by exfoliation from bulk graphite samples in 2004 and the experimental investigation of its transport properties.[1] The observation of a half-integer quantum-Hall effect indicated the presence of relativistic charge carriers.[2,3] Its relation to the Klein paradoxon and its high carrier mobility of 1.5×10^4 cm^2/Vs (Ref. 4) made the physics of quasiparticles in graphene a subject of intensive spectroscopic research.[5] It was possible to directly measure the band dispersion of massless Dirac fermions for graphene grown on SiC (Ref. 6) and on Ni(111) after intercalation of one monoatomic layer (ML) of Au.[7] Band-gap control at the Dirac point was demonstrated for graphene bilayers on SiC by the electric field of adsorbed alkali atoms, thus adding to the perspectives of a carbon-based electronics.[8,9]

The application of spintronic concepts to graphene suggests further possibilities of accelerated signal processing. The huge potential of graphene for spintronics has been demonstrated in a recent work which evidenced a μm scale of spin-relaxation length at room temperature caused by weak spin-orbit interaction in this material.[4] Another key prerequisite for the use of graphene in spintronics are ferromagnetic contacts. A 10% change in magnetoresistance was observed at room temperature for graphene attached to Permalloy and has been interpreted as spin injection.[10]

The classical method of micromechanical cleaving[1,2] appears inadequate for a reliable fabrication of such graphene-based spintronic devices. Therefore, epitaxial growth of graphene by chemical vapor deposition, i.e., cracking of hydrocarbons at Ni surfaces,[11,12] has recently been considered. This fabrication method by self-organization provides graphene layers of extremely high quality with significantly reduced defect density as compared to graphitized SiC substrates (see, e.g., Refs. 13–15 for graphene on SiC and Refs. 16 and 17 for graphene on metals).

In the context of graphene spintronics, an experiment recently conducted by Dedkov *et al.*[18] on chemical-vapor-deposited graphene on Ni attracted considerable interest. An intriguing magnetic effect—a $k_\parallel$ shift of the graphene π band upon reversal of the magnetization of the Ni substrate—was observed in angle-resolved photoemission measurements. The origin of the shift was attributed to a spin polarization induced in graphene through hybridization of its π states with spin-polarized $3d$ states of Ni. It was assumed that the Rashba-type spin-orbit interaction[19] caused by a large potential gradient at the Ni-graphene interface affects the electron spin in graphene and that it can be influenced by switching the magnetization of the Ni substrate. Ref. 18 discusses the observed $k_\parallel$ shift of the π band in the framework of a concept suggested by Krupin *et al.*[20] for the observation of a magnetization-dependent Rashba effect in photoemission without the need for spin resolution. We have recently shown by spin-resolved photoemission that the spin polarization of graphene π states is too low and the spin-orbit interaction too small for this effect to be observed in graphene/Ni and graphene/Co (Ref. 21) while, after intercalation of 1 ML Au between graphene and Ni(111), a Rashba effect with a spin-orbit splitting of ~13 meV can be observed.[7,22] Presently, the magnetotransport properties of graphene/Permalloy[4] still await explanation and it is possible that the observations in Ref. 18, while not being of Rashba origin, are related to them.

In order to gain understanding of the magnetic effect demonstrated in Ref. 18, we investigate graphene on a ferromagnetic surface which has a magnetic moment larger than that of Ni. For this purpose we developed a technique for epitaxial growth of graphene on Co(0001). Similar to the case of Ni,[7,18] graphene was prepared by chemical vapor deposition using propylene and a moderately hot (450 °C) Co(0001) film grown before on a W(110) substrate. The partial pressure of propylene during graphene formation was 1×10^{-6} mbar. Graphene deposition is a self-limiting process which terminates upon formation of a single atomic layer of graphene. The magnetic spin moment of Co

($1.76\mu_B$/atom) is approximately three times larger than that of Ni ($0.615\mu_B$/atom). Hence, if the magnetic effect observed previously is related to graphene-substrate interaction,[18] the magnitude of the $k_\parallel$ shift may as well be larger for graphene/Co than for graphene/Ni.

II. EXPERIMENTAL

Angle-resolved photoemission experiments have been performed with a hemispherical electron-energy analyzer and linearly polarized undulator radiation at the UE112-PGM1 and PGM2b beamlines of BESSY II. For spin analysis, a Rice University Mott-type spin polarimeter has been operated at 26 kV.[23] The spin-quantization axis lies in the surface plane of the sample, parallel to the magnetization direction **M** of the sample, see Fig. 2(b). We developed a special sample manipulator optimized for spin- and angle-resolved photoemission.[24] The manipulator is fully automated and computer controlled. Its accuracy of sample positioning is 50 μm and 0.1° for sample translations and rotations, respectively. The manipulator is equipped with integrated Helmholtz coils which were used to generate magnetic field pulses in the sample surface plane and to remanently magnetize the sample. This can be done without changing any axis coordinates. Analogous to Ref. 18, we investigated how the dispersion of the π band in graphene/Co(0001), measured along the direction perpendicular to the remanent magnetization of Co film, changes upon magnetization reversal. Due to the fact that the easy axis of magnetization in Co(0001)/W(110) is aligned to $[1\bar{1}00]$ which corresponds to the $\overline{\Gamma M}$ direction of the graphene Brillouin zone, we measured the π-band dispersion along the $\overline{\Gamma K}$ direction. For details see Fig. 2(b).

III. RESULTS

A. Characterization of graphene/Co(0001)

The structural quality and electronic properties of graphene fabricated on bulklike Co(0001)/W(110) were investigated by low-energy electron diffraction (LEED) and scanning tunneling microscopy (STM) in Fig. 1 and by angle-resolved photoemission in Fig. 2. Figure 1(a) shows the twofold-symmetric LEED pattern from W(110). 15 ML Co/W(110) as deposited show the sixfold-symmetric LEED pattern of Fig. 1(b). Figure 1(c) displays the LEED pattern from this sample after chemical vapor deposition of graphene. It indicates a predominant $p(1\times1)$ structure in registry with the Co substrate plus weaker circle segments indicating domains of graphene slightly rotated relative to the Co lattice. A similar pattern is seen for graphene/Ni(110).[25] Figure 1(d) displays a large-scale STM image of graphene/Co(0001) and reveals the formation of a perfect honeycomb structure. Figure 1(e) shows a fine-scale STM image of graphene/Co(0001) with the unit cell of ideal graphene superimposed. One clearly sees the threefold symmetry similar to the case of graphene on the (111) face of Ni.[7] These observations are consistent with the structural model in Fig. 2(a) suggested also for graphene/Ni(111).[26,27]

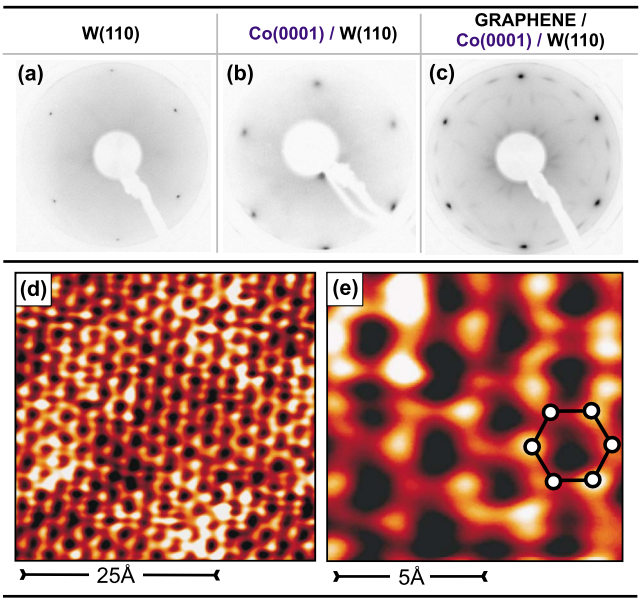

FIG. 1. (Color online) Preparation and structure of graphene on Co(0001). LEED patterns from (a) bare W(110), (b) 15 ML Co/W(110), and (c) graphene/15-ML Co/W(110). (d) The STM characterization of graphene/Co(0001) reveals the formation of high-quality graphene with (e) pronounced threefold symmetry in the spatial electronic structure.

The high quality of graphene/Co(0001) and the similarity of its electronic structure to the one of graphene on Ni(111) are verified by angle-resolved photoemission measurements. Figure 2(c) reveals characteristic dispersions of π and σ states in the valence band. Comparing graphene/Co(0001) to graphene/Ni(111) near the $\bar{K}$ point, we see that contributions from other directions of the surface Brillouin zone (SBZ) are superimposed, which correspond to the extra structures seen by LEED. Otherwise, critical-point energies of π and σ states in graphene/Co(0001) are nearly the same as in graphene/Ni(111). This means, in particular, that properties of the bonding between graphene and its ferromagnetic substrate such as the amount of charge transfer and overlayer-substrate hybridization are very similar for Co(0001) and Ni(111).

B. Graphene on separate Co(0001) islands

In order to be able to separate intrinsic magnetic effects from the influence of environmental magnetic fields on the photoemitted electron, we have prepared the sample in a particular way which allows us to obtain a reference for an absolute determination of angular and momentum coordinates of photoemission from graphene bands relative to the sample surface. First of all, we made use of the fact that in contrast to Ni, the Co layer is rather unstable on W(110) and can easily be broken up into microscopic islands by annealing above 600 °C.[28] (This preparation will further on be referred to as "overannealing.") The fact that photoemission is a nonlocal probe, i.e., it averages in our case over an area of ~0.1 mm^2, allows us to measure the dispersion of *sp* bands of open W(110) areas between Co islands *simultaneously*

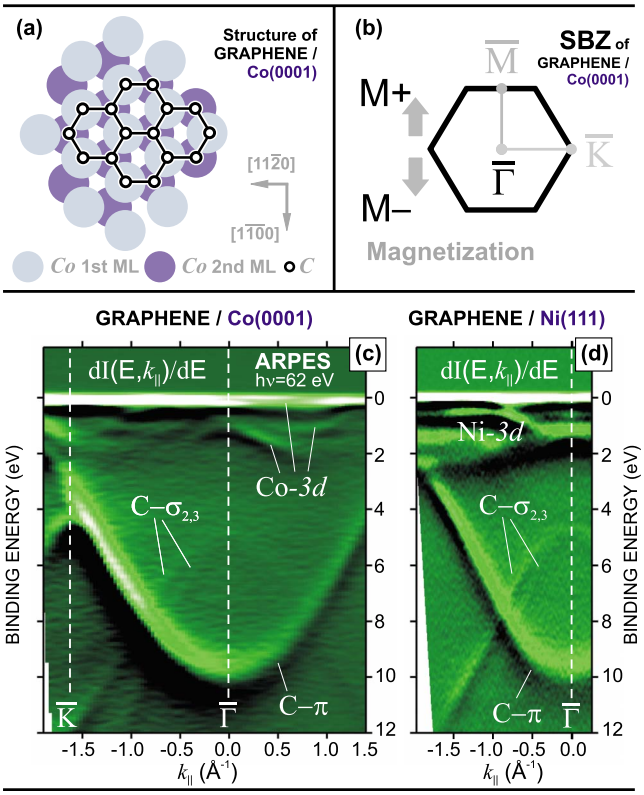

FIG. 2. (Color online) (a) Structural model of graphene on Co(0001).(b) SBZ of graphene and directions of Co magnetization. (c) Angle-resolved photoemission of the band structure of graphene/Co(0001) along $\bar{\Gamma}\bar{K}$ as compared to the band structure of (d) graphene on Ni(111).

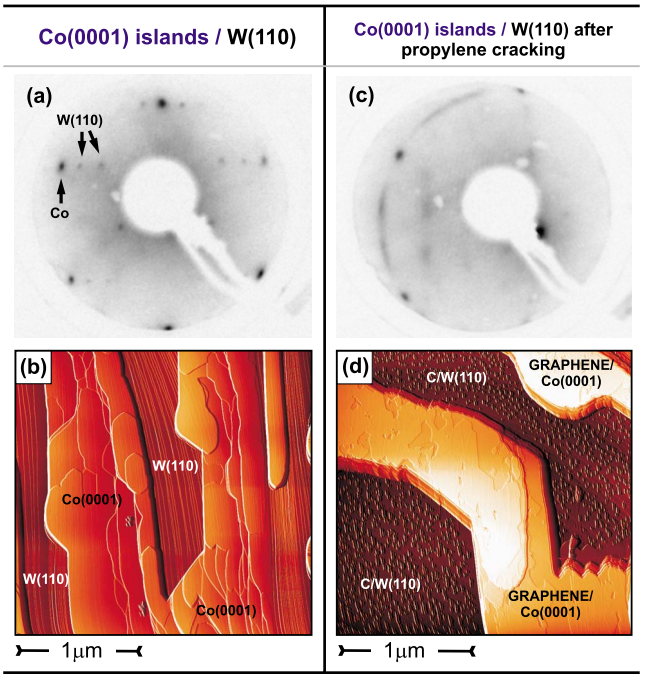

FIG. 3. (Color online) Characterization of a Co film collapsed into three-dimensional islands. (a) LEED and (b) STM from an overannealed 15 ML Co film. LEED (c) and STM (d) from the same sample after graphene formation.

with the dispersion of π bands of graphene on magnetized Co islands.

The effect of breaking the Co film up was studied by means of LEED and STM for 15 ML Co/W(110) and the detailed results are presented in Fig. 3. Figures 3(a) and 3(b) characterize the broken Co films before graphene preparation. The LEED pattern in Fig. 3(a) clearly indicates the coexistence of diffraction patterns from Co(0001) and W(110) suggesting the presence of open W(110) surfaces between Co islands. This conclusion is confirmed by the STM measurements in Fig. 3(b). They reveal that the overannealed Co film collapses into three-dimensional islands which are 6–8 nm high and separated by large areas of the W(110) substrate. These areas can be identified as open sites of W(110) due to the presence of long and straight monoatomic steps characteristic of the bare W(110).

We subsequently performed graphitization of the Co film collapsed into three-dimensional islands. Results of the structural characterization by means of LEED and STM are shown in Figs. 3(c) and 3(d), respectively. LEED indicates the appearance of typical graphene ring sections mentioned above, while the STM reveals that the character of phase separation between Co and W(110) remains unaffected. Fine-scale STM measurements of the island surface (not shown) indicate the formation of a graphene layer identical to the one shown in Fig. 1(e). Areas between three-dimensional islands demonstrate the formation of clusters consisting possibly of amorphous carbon on top of the flat W(110) surface carbide.

The assumption that areas between three-dimensional Co islands are Co-free sites of W(110) is further confirmed by photoemission measurements of the chemically sensitive W 4f core level. Figure 4(a) presents the W 4f spectrum of W(110) covered by a *continuous* 3-ML-thick Co film. The W $4f_{7/2}$ peak at 31.4 eV binding energy is clearly accompanied by an additional peak at 32.1 eV, which can be ascribed to the W-Co interface. In contrast, the W 4f peak from an overannealed 15-ML-thick Co film does not indicate any interface component after graphene deposition but shows just a shoulder at 31.6 eV, which can be ascribed to the initial stage of formation of a defect-rich tungsten surface carbide.[29] The absence of the interface component from the spectrum shown in Fig. 4(b) unambiguously confirms that open areas between Co islands are W(110) and do not bear any continuous Co film on top. The strong dispersion of W bands is used as a reference for the determination of angular and momentum coordinates of electrons photoemitted from the sample, in particular, for identifying normal emission.

C. Magnetization dependence

The spectra in Figs. 4(c) and 4(d) emphasize the difference between valence-band photoemission from graphitized uncollapsed [Fig. 4(c)] and collapsed [Fig. 4(d)] Co films on W(110). The presented spectra were measured angle resolved and off normal for an emission angle of $\theta=-8.5°$ ($k_{||}=-0.54$ Å^{-1}). While for the continuous Co layer [Fig. 4(c)] only characteristic π states of graphene (9.5 eV) along

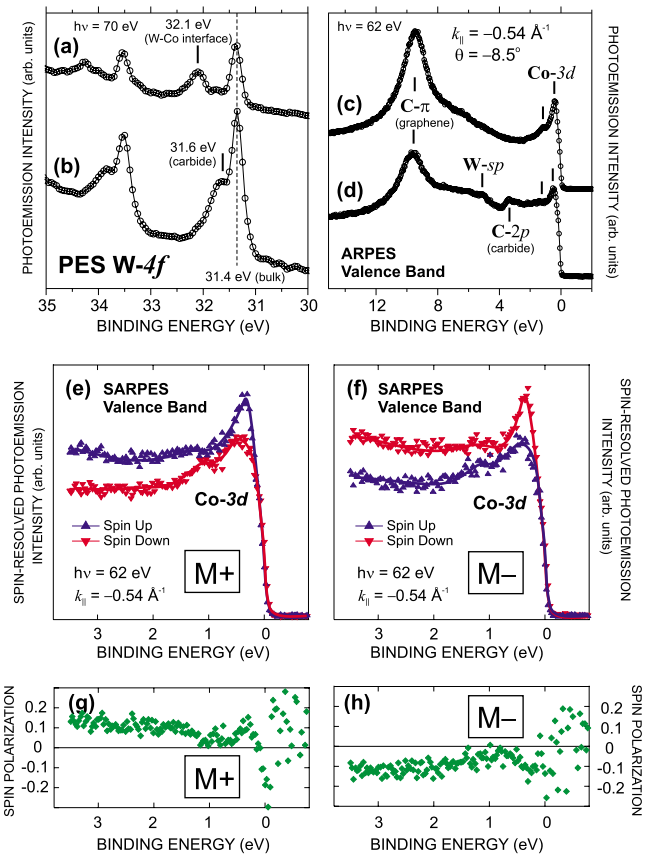

FIG. 4. (Color online) [(a)–(d)] Comparison of photoemission from the sample with continuous and broken-up Co layer. For the continuous Co film, the (a) 4*f* core-level spectrum of the W substrate reveals an intense interface component, and the (c) valence band shows graphene and Co states only. (b) When Co is overannealed and collapses into three-dimensional islands, the interface component of W 4*f* is not observed any longer and (d) in the valence band, W-derived peaks appear. For this broken and graphene-covered Co film, [(e)–(h)] spin-resolved spectra of the energy range of Co 3*d* states measured for opposite magnetization directions confirm reversal of the remanent magnetization.

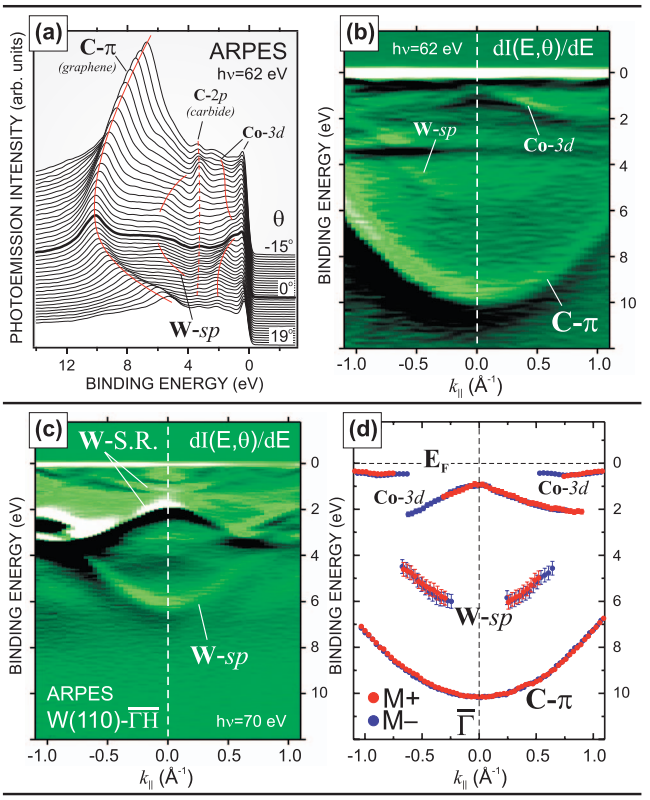

FIG. 5. (Color) Photoemission verification of the $k_{\parallel}$ shift of the graphene π band upon magnetization reversal. (a) Raw data and (b) first derivative of valence-band photoemission intensity measured from 15 ML Co/W(110) graphitized and collapsed into three-dimensional islands. Dispersing bands of bulk Co and bulk W are clearly visible and are used as reference for angular and momentum distribution of photoelectrons from graphene. (c) The measured band structure of clean W(110) confirms the correct identification of W *sp* states in (a) and (b). (d) $E(k_{\parallel})$ diagram containing fitted positions of photoemission peaks of graphene, Co, and W measured for opposite directions of Co magnetization. No $k_{\parallel}$-shift effect is detected.

with 3*d* states of Co (0–3 eV) are seen, for the Co layer collapsed into islands, additional peaks originating from W appear at binding energies between 3 and 7 eV. The superimposed band structures of such a graphene-covered sample with a collapsed Co film on top are shown in more detail in Figs. 5(a) and 5(b). Figure 5(a) demonstrates the emission-angle dependence of the spectra. The intensity from W bulk *sp* bands is rather weak due to the coverage of the W(110) surface with carbide. In order to emphasize these weak peaks, Fig. 5(b) presents the first derivative of the measured photoemission intensity.

To show that our identification of the features at 3–7 eV binding energy as W bands is correct, we display in Fig. 5(c) the band structure of clean W(110) mapped for the same experimental geometry as in Figs. 5(a) and 5(b). Although the valence-band spectra are dominated by photoemission peaks from surface resonances (denoted as W-SR),[30,31] the dispersion of the bulk *sp* band of W is clearly seen between 3 and 7 eV and is fully consistent with the dispersion observed in Fig. 5(b). A weakly dispersing peak at ~3.4 eV can be attributed to the formation of tungsten surface carbide.

Another reference available for the analysis of magnetization-dependent $k_{\parallel}$ shifts of the graphene π band is the dispersion of the Co 3*d* band, which is clearly observed at binding energies between 1 and 3 eV [Figs. 2(c), 5(a), and 5(b)]. To distinguish these peaks from possible graphene-Co interface states, as have been predicted for graphene/Ni(111),[27] we studied their photon-energy dependence. The peaks in question are identified as Co bulk states because they exhibit a $k_{\perp}$ dispersion with photon energy and because they also appear for nongraphitized Co(0001).

Measuring graphitized overannealed Co films on W(110) and taking advantage of the dispersion of W *sp* and Co 3*d* bands for calibration of the angular scale of photoemitted electrons, we tested precisely how the $E(k_{\parallel})$ dispersion of the graphene π band behaves upon magnetization reversal of the broken Co(0001). Reversal of the remanent magnetization, which is essential for our conclusions, was conducted by

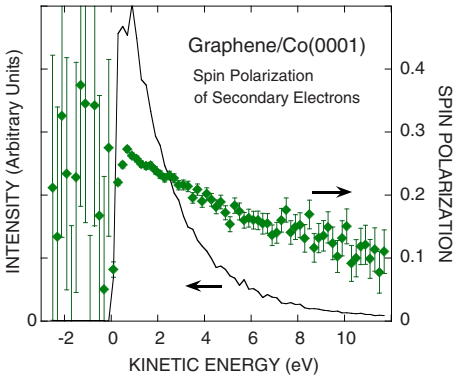

FIG. 6. (Color online) Spin-resolved photoemission of secondary electrons of graphene/Co(0001) as a continuous film. High spin-polarization values of up to ~25% are observed near the cutoff and are due to the Co underneath the graphene.

applying a magnetic pulse and verified by means of spin-resolved photoemission. Figures 4(e)–4(h) show spin- and angle-resolved spectra of the broken and graphene-covered Co film as well as the spin polarization in the energy range of Co 3*d* states for both magnetization directions $\mathbf{M}^+$ and $\mathbf{M}^-$. The spectra were measured off normal at an emission angle of $\theta=-8.5°$ with an angular-analyzer acceptance of 3° to accelerate data aquisition for our purpose. The spectra correspond to the spin-averaged spectrum shown in Fig. 4(d). The reversal of spin polarization of exchange-split Co 3*d* bands and hence the reversal of the substrate magnetization is clearly demonstrated.

The diagram in Fig. 5(d) contains fitted positions of valence-band peaks dispersing along the $\overline{\Gamma K}$ direction of the graphene Brillouin zone measured for opposite Co magnetizations. The result for the graphene/Co(0001) system is that we do not observe any $k_\parallel$ shift of the graphene π band neither relative to W *sp* bands nor relative to Co 3*d* bands. The error margin of this result is determined by the accuracy of peak fitting and allows for a maximally possible shift of $\Delta k_\parallel=0.008$ Å^{-1} which is ten times smaller than the effect reported in Ref. 18 for graphene/Ni(111).

Graphene/Ni(111) was recently suggested by Dedkov *et al.*[32] as inert source of spin-polarized electrons due to its stability against high doses of oxygen. A spin polarization of the secondary electrons of up to ~12% was measured and assigned to the Ni spin polarization slightly reduced at the interface with graphene.[32] This result is principally confirmed by our data from graphene/Co(0001) films in Fig. 6. The spin polarization of secondary electrons excited by photons of 56 eV rises, as usual, for kinetic energies in the range of the *d*-band width. Spin-polarization values of up to ~25% are obtained due to the larger magnetic moment of Co.

IV. SUMMARY

We developed a technique for synthesis of graphene on a Co(0001) substrate. Our extensive characterization of this system by spectroscopic and microscopic techniques reveals that it is nearly identical to graphene on Ni(111), both structurally and electronically and that, in addition, graphene-covered Co(0001) islands can be grown on W(110) separated by substrate areas free of Co and graphene. For these samples, we examined the magnetic effect on the band dispersion recently reported[18] for graphene on Ni(111) and found that such effect does not exist for graphene on Co(0001). We confirmed that graphene does not strongly diminish the spin polarization from secondary electrons from the underlying ferromagnet with values of up to ~25% measured for graphene/Co(0001).

[1] K. S. Novoselov, A. K. Geim, S. V. Morozov, D. Jiang, Y. Zhang, S. V. Dubonos, I. V. Grigorieva, and A. A. Firsov, Science **306**, 666 (2004).
[2] K. S. Novoselov, A. K. Geim, S. V. Morozov, D. Jiang, M. I. Katsnelson, I. V. Grigorieva, S. V. Dubonos, and A. A. Firsov, Nature (London) **438**, 197 (2005).
[3] Y. Zhang and Y.-W. Tan, H. L. Stormer, and Philip Kim, Nature (London) **438**, 201 (2005).
[4] N. Tombros, C. Jozsa, M. Popinciuc, H. T. Jonkman, and B. J. van Wees, Nature (London) **448**, 571 (2007).
[5] M. I. Katsnelson, K. S. Novoselov, and K. Geim, Nat. Phys. **2**, 620 (2006).
[6] A. Bostwick, T. Ohta, T. Seyller, K. Horn, and E. Rotenberg, Nat. Phys. **3**, 36 (2007).
[7] A. Varykhalov, J. Sánchez-Barriga, A. M. Shikin, C. Biswas, E. Vescovo, A. Rybkin, D. Marchenko, and O. Rader, Phys. Rev. Lett. **101**, 157601 (2008).
[8] T. Ohta, A. Bostwick, T. Seyller, K. Horn, and E. Rotenberg, Science **313**, 951 (2006).
[9] E. V. Castro, K. S. Novoselov, S. V. Morozov, N. M. R. Peres, J. M. B. Lopes dos Santos, J. Nilsson, F. Guinea, A. K. Geim, and A. H. Castro Neto, Phys. Rev. Lett. **99**, 216802 (2007).
[10] S. Sahoo, T. Kontos, J. Furer, C. Hoffmann, M. Gräber, A. Cottet, and C. Schönenberger, Nat. Phys. **1**, 99 (2005).
[11] K. Yamamoto, M. Fukushima, T. Osaka, and C. Oshima, Phys. Rev. B **45**, 11358 (1992).
[12] A. M. Shikin, G. V. Prudnikova, V. K. Adamchuk, F. Moresco, and K.-H. Rieder, Phys. Rev. B **62**, 13202 (2000).
[13] G. M. Rutter, J. N. Crain, N. P. Guisinger, T. Li, P. N. First, and J. A. Stroscio, Science **317**, 219 (2007).
[14] N. P. Guisinger, G. M. Rutter, J. N. Crain, C. Heiliger, P. N. First, and J. A. Stroscio, J. Vac. Sci. Technol. A **26**, 932 (2008).
[15] Th. Seyller, K. V. Emtsev, K. Gao, F. Speck, L. Ley, A. Tadich, L. Broekman, J. D. Riley, R. C. G. Leckey, O. Rader, A. Varykhalov, and A. M. Shikin, Surf. Sci. **600**, 3906 (2006).
[16] D. Usachov, A. M. Dobrotvorskii, A. Varykhalov, O. Rader, W. Gudat, A. M. Shikin, and V. K. Adamchuk, Phys. Rev. B **78**, 085403 (2008).
[17] B. Wang, M.-L. Bocquet, S. Marchini, S. Gunther, and J. Wintterlin, Phys. Chem. Chem. Phys. **10**, 3530 (2008).
[18] Yu. S. Dedkov, M. Fonin, U. Rüdiger, and C. Laubschat, Phys. Rev. Lett. **100**, 107602 (2008).

[19] E. I. Rashba, Fiz. Tverd. Tela (Leningrad) **2**, 1224 (1960) [Sov. Phys. Solid State **2**, 1109 (1960)].
[20] O. Krupin, G. Bihlmayer, K. Starke, S. Gorovikov, J. E. Prieto, K. Döbrich, S. Blügel, G. Kaindl, Phys. Rev. B **71**, 201403(R) (2005); O. Krupin, G. Bihlmayer, K. M. Döbrich, J. E. Prieto, K. Starke, S. Gorovikov, S. Blügel, S. D. Kevan, and G. Kaindl, New J. Phys. **11**, 013035 (2009).
[21] O. Rader, A. Varykhalov, J. Sánchez-Barriga, D. Marchenko, A. Rybkin, and A. M. Shikin, Phys. Rev. Lett. **102**, 057602 (2009).
[22] E. I. Rashba, Phys. Rev. B **79**, 161409(R) (2009).
[23] G. C. Burnett, T. J. Monroe, and F. B. Dunning, Rev. Sci. Instrum. **65**, 1893 (1994).
[24] Details of Pente.Ax manipulator will be given in A. Varykhalov, (unpublished).
[25] A. M. Shikin, S. A. Gorovikov, V. K. Adamchuk, W. Gudat, and O. Rader, Phys. Rev. Lett. **90**, 256803 (2003).
[26] R. Rosei, M. De Crescenzi, F. Sette, C. Quaresima, A. Savoia, and P. Perfetti, Phys. Rev. B **28**, 1161 (1983).
[27] G. Bertoni, L. Calmels, A. Altibelli, and V. Serin, Phys. Rev. B **71**, 075402 (2005).
[28] J. Bansmann, L. Lu, V. Senz, A. Bettac, M. Getzlaff, and K. H. Meiwes-Broer, Eur. Phys. J. D **9**, 461 (1999).
[29] A. Varykhalov, O. Rader, and W. Gudat, Phys. Rev. B **72**, 115440 (2005).
[30] R. H. Gaylord and S. D. Kevan, Phys. Rev. B **36**, 9337 (1987).
[31] J. Feydt, A. Elbe, H. Engelhard, G. Meister, Ch. Jung, and A. Goldmann, Phys. Rev. B **58**, 14007 (1998).
[32] Yu. S. Dedkov, M. Fonin, and C. Laubschat, Appl. Phys. Lett. **92**, 052506 (2008).